Carrier transport mechanism in the SnO_2:F/p-type a-Si:H heterojunction

G. Cannella,[1,2,a)] F. Principato,[1] M. Foti,[3] S. Di Marco,[3] A. Grasso,[3] and S. Lombardo[2]
[1]*Dipartimento di Fisica, University of Palermo, Building 18, Viale delle Scienze, 90128 Palermo, Italy*
[2]*CNR-IMM, Ottava Strada, 5, Zona Industriale, 95121 Catania, Italy*
[3]*STMicroelectronics, Stradale Primosole, 50, 95121 Catania, Italy*

(Received 9 December 2010; accepted 25 May 2011; published online 19 July 2011)

We characterize SnO_2:F/p-type a-Si:H/Mo structures by current-voltage (I-V) and capacitance-voltage (C-V) measurements at different temperatures to determine the transport mechanism in the SnO_2:F/p-type a-Si:H heterojunction. The experimental I-V curves of these structures, almost symmetric around the origin, are ohmic for $|V|<0.1$ V and have a super-linear behavior (power law) for $|V|<0.1$ V. The structure can be modeled as two diodes back to back connected so that the main current transport mechanisms are due to the reverse current of the diodes. To explain the measured C-V curves, the capacitance of the heterostructure is modeled as the series connection of the depletion capacitances of the two back to back connected SnO_2:F/p-type a-Si:H and Mo/p-type a-Si:H junctions. We simulated the reverse I-V curves of the SnO_2:F/p-type a-Si:H heterojunction at different temperatures by using the simulation software SCAPS 2.9.03. In the model the main transport mechanism is generation of holes enhanced by tunneling by acceptor-type interface defects with a trap energy of 0.4 eV above the valence bandedge of the p-type a-Si:H layer and with a density of 4.0×10^{13} cm^{-2}. By using I-V simulations and the proposed C-V model the built-in potential (V_{bi}) of the SnO_2:F/p-type a-Si:H (0.16 V) and p-type a-Si:H/Mo (0.14 V) heterojunctions are extracted and a band diagram of the characterized structure is proposed. © *2011 American Institute of Physics*. [doi:10.1063/1.3606408]

I. INTRODUCTION

The thin film silicon solar cells have raised considerable interest because the a-Si:H thin film technology is very simple and inexpensive and it is used on large area and low-cost substrates. In a thin film amorphous silicon solar cell the window layer is typically made with a p-type a-Si:H or p-type a-SiC:H film deposited onto a transparent conductive oxide (TCO). This heterojunction plays an important role on the solar cell performance and many authors have studied this interface.[1–6]

In an a-Si:H solar cell there are two possibilities to improve the electronic performances of the window layer: using a better p-type semiconductor or a better TCO. In the former case the literature proposes to replace the a-Si:H material with either a-SiC:H, because it has a higher bandgap and a lower light absorption, or with microcrystalline Silicon (μc-Si), which has a lower contact resistance.[7] The latter possibility proposes typically two types of TCOs: highly doped tin oxide (SnO_2) and highly doped zinc oxide (ZnO).[8] To increase the conversion efficiency of the solar cells the electrical and the radiation losses of the TCO have to be reduced.[9] The textured SnO_2:F is an industry standard for superstrate (glass/TCO/p-i-n/metal) type a-Si:H solar cells,[10] because it has a lot of advantages compared to other TCOs, as the lowest plasmon frequency, the highest work function (good for p-type a-Si contacts), an excellent thermal stability, mechanical and chemical durability, the lowest cost and toxicity.[8] Although the workfunction of the SnO_2:F is greater than that of the ZnO:Al, solar cells deposited on SnO_2 exhibit a reduced short circuit current density compared to that of the solar cells deposited on doped ZnO.[11] This reduction is probably due to the formation of a damaged layer at the TCO/p-type a-Si:H interface caused by the hydrogen plasma discharge.[11] Hence, the characterization of the TCO/p-type a-Si:H interface is crucial to improve the performances of amorphous solar cell structures.[8–11]

The aim of this work is to understand the carrier transport mechanism of the SnO_2:F/p-type a-Si:H heterojunction. This heterojunction is an anisotype n^+-p junction with type 2 alignment of the band levels. Many authors have studied this structure, using both experimental methods[3,4] and numerical simulations.[1,5] Sinencio[3] and Itoh[4] have experimentally studied the heterojunctions SnO_2/p-type a-Si:H and SnO_2/p-type a-SiC, respectively, and have determined the Schottky barrier height measuring the short circuit current and open circuit voltage under illumination and by using the pulsed laser-induced transient photopotential technique. In both cases the carrier transport has not been investigated. The theory of thermionic and thermionic-field emission, valid for metal-semiconductor contacts, has been applied for metal/a-Si:H contacts,[12,13] but this theory cannot explain the non rectifying behavior of TCO/p-type a-Si:H heterojunctions, such as the ZnO:Al/p-type a-Si:H.[7]

In order to characterize the SnO_2:F/p-type a-Si:H heterojunction we have performed C-V and I-V measurements, in dark and at different temperatures, of the SnO_2:F/p-type a-Si:H/Mo structures, which shows high current levels without rectifying behavior. Due to the high doping density of the

a)Author to whom correspondence should be addressed. Electronic mail: giuseppe.cannella@imm.cnr.it.

 © 2011 American Institute of Physics

Author complimentary copy. Redistribution subject to AIP license or copyright, see http://jap.aip.org/jap/copyright.jsp

SnO_2 layer, the contact resistance of the SnO_2:F/p-type a-Si:H heterojunction is comparable with that of the Mo/p-type a-Si:H Schottky junction, which is used as electrical probe. This issue is taken into account in the C-V and I-V analysis with a combination of analytical modeling and numerical simulation of charge transport performed through the SCAPS 2.9.03 (Ref. 14) simulation program.

II. MATERIALS AND METHODS

The investigated SnO_2:F/p-type a-Si:H/Mo structures were fabricated by STMicroelectronics (Catania, Italy). The a-Si:H was deposited by plasma-enhanced chemical vapor deposition (PECVD) of SiH_4 and Trimethyl borane (TMB) with a ratio TMB:SiH_4 of 1:100, diluted with 10% of hydrogen and at a temperature of 255 °C on 800 nm thick SnO_2:F film on 6" glass substrates produced by AGC ASAHI GLASS. The thickness of the p-type a-Si:H layer is either 20 nm or 100 nm. An additional 800 nm thick Molybdenum film on the p-type a-Si:H layer was deposited by sputtering. The final geometries were defined by photolithography and selective etching. The structures used in this work are schematically shown in the inset of Fig. 1. The geometry is circular, with the following diameters: 0.01, 0.02, 0.04, 0.08, 0.16, 0.32, and 0.64 cm.

The structures were characterized by measuring the current density versus voltage (J-V) curves with the four-point probe technique. The J-V curves were measured with the bias voltage varying in the $[-0.40, 0.40]$ V range by using a Keithley 236.

The film sheet resistance of the p-type a-Si:H was measured by using the four-point probe technique under vacuum, in dark and at different temperatures (300 to 600 K). The experimental details can be found in Ref. 15.

The capacitance-voltage (C-V) measurements were performed using a Keithley 4980A LCR meter in four terminal (4TP) configuration and with the voltage bias varying from -0.1 up to $+0.1$ V, where the low current levels flowing into the devices allow to measure the capacitance with a good precision. The ac oscillator amplitude used is 30 mV at the frequency of 1 MHz to neglect the effect of the traps.

All J-V and C-V measurements were taken in dark and at different temperatures (from 303 to 353 K with step of 10 K), in N_2 atmosphere, by using a Peltier temperature controller.

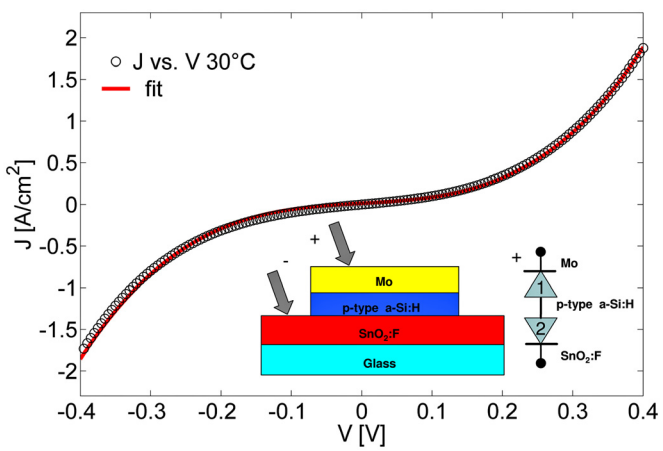

FIG. 1. (Color online) Comparison between the measured (black circle) J-V curve and the cubic law ($J = a \cdot V^3 + b$-V) fitting (red line) of the SnO_2:F/p-type aSi:H/Mo structure at 30 °C. The samples have a diameter of 0.02 cm. In the inset is shown the structure under investigation and the diode configuration. The positive bias is applied to Molybdenum.

III. CAPACITANCE MODEL OF BACK TO BACK SERIES CONNECTED JUNCTIONS

Generally, for a Schottky junction the C-V curves can be used to determine the doping density N_A and the built-in potential V_{bi}. In this case the depletion layer capacitance as a function of the applied bias V is $C = (q\varepsilon N_A/2(V_{bi} - V - V_T))^{1/2}$, where q is the electron charge, ε is the dielectric constant of the depletion layer, $V_T = kT/q$ is the thermal voltage, k is the Boltzmann constant and T is the temperature in Kelvin. In our case, the device consists of two back-to-back connected junctions, the Mo/p-type a-Si:H and the p-type a-Si:H/n^+-SnO_2:F, denoted with the labels 1 and 2, respectively, as shown in the inset of Fig. 1. Denoting with V_1 and V_2 the voltage drops across the two junctions, with $V_{bi,1}$ and $V_{bi,2}$ the respective built-in potentials, and neglecting the potential drops across the p-type a-Si:H film, it results that $V = V_1 + V_2$, where V is the externally applied bias. The built-in potential of each junction can expressed as $V_{bi,i} = \phi_{B,i} - E_A$, where $i = 1,2$, $\phi_{B,i}$ is the barrier height of the junction which takes into account also the interface states contribution,[16,17] and E_A is the distance between Fermi level and valence bandedge in the quasi neutral region of the p-type a-Si:H layer, approximately equal to the activation energy of the electrical conductivity of this layer.

The capacitance of the two depleted boundary layers assuming abrupt junctions are $C_1 = (q\varepsilon N_A/2(V_{bi,1} + V_1 - V_T))^{1/2}$ and $C_2 = (q\varepsilon N_A/2(V_{bi,2} - V_2 - V_T))^{1/2}$, respectively. Here, we assume that V is positive when the potential at the Mo layer is higher than that of the SnO2:F contact. Hence, when V is positive, assuming V_1 and V_2 also with positive sign, then the Mo/p-type a-Si:H is reverse biased whereas the p-type a-Si:H/SnO_2:F junction is forward biased. In order to find the expression of the voltages V_1 and V_2 as a function of V, we consider that for low voltages, if the barriers are ohmic, the currents flowing in each junction are governed by tunneling and can be described as $J_i = K_{0,i} \exp(-\phi_{B,i}/V_T) \cdot V_i$,[18] where $K_{0,i}$ depends on temperature and on doping.

The currents flowing into each junction must be equal and considering $K_{0,1}/K_{0,2} \cong 1$, we obtain:

$$\frac{V_1}{V_2} = \frac{\exp(-\phi_{B,2}/V_T)}{\exp(-\phi_{B,1}/V_T)} = \frac{\exp(-V_{bi,2}/V_T)}{\exp(-V_{bi,1}/V_T)}$$

Hence, using the relation $V = V_1 + V_2$ and the previous equation we have $V_1 = V \cdot F(V_{bi,1}, V_{bi,2})$ and $V_2 = V \cdot (1 - F(V_{bi,1}, V_{bi,2}))$, where

$$F(V_{bi,1}, V_{bi,2}) = \frac{1}{1 + \exp\left[\frac{(V_{bi,2} - V_{bi,1})}{V_T}\right]}.$$

The depletion layer capacitance C of the structure is the series connection of the two capacitances C_1 and C_2, which can expressed as a function of the applied voltage V as

Author complimentary copy. Redistribution subject to AIP license or copyright, see http://jap.aip.org/jap/copyright.jsp

$$C = \sqrt{\frac{qN_A\varepsilon}{2}} \frac{1}{\sqrt{V_{bi,1} + V \cdot F\left(V_{bi,1}, V_{bi,2}\right) - V_T} + \sqrt{V_{bi,2} - V \cdot \left[1 - F\left(V_{bi,1}, V_{bi,2}\right)\right] - V_T}} \quad (1)$$

When the values of the built-in voltages are comparable the capacitance C and $1/C^2$ are both nonlinear function of the applied voltage V, i.e. the intercept method[18] to determine the built-in potential and the doping profile can not be used. For fixed value of N_A, it results that the expression of capacitance (Eq. (1)) is a monotonic decreasing or increasing function of the voltage, depending on the sign of the difference $(V_{bi,2} - V_{bi,1})$. Fig. 2 shows the C-V curves obtained from expression (Eq. (1)) for three different values of the difference $\Delta V_{bi} = (V_{bi,2} - V_{bi,1})$. We note that for $\Delta V_{bi} = 0$ the C-V curve is constant, whereas for $\Delta V_{bi} > 0$ $(\Delta V_{bi} < 0)$ the capacitance is a increasing (decreasing) function of the voltage.

IV. MEASUREMENTS ON THE SnO_2:F/P-TYPE a-Si:H HETEROJUNCTION

As preliminary analysis, we have characterized the sheet resistance of the p-type a-Si:H and SnO_2:F layers and the effect of the TCO distributed resistance on the electrical measurements. We have measured the sheet resistance and the activation energy of the resistivity of both the SnO_2:F and the p-type a-Si:H layers. The measured sheet resistance of the SnO_2:F layer is 8.8 ± 0.2 Ω/□, and does not depend on the temperature. From the value of the resistivity, we have extracted the doping $N_D = 2.9 \pm 0.1 \times 10^{20}$ cm^{-3} of the SnO_2:F layer, by assuming a value of the electron mobility equal to 30 cm^2/Vs.[1]

The measured value of the p-type a-Si:H activation energy is about 0.38 eV and the resistivity at room temperature is about 2.0×10^4 Ωcm.[15]

The investigated samples consists of two back-to-back connected junctions: Mo/p-type a-Si:H and p-type a-Si:H/SnO_2:F as shown in the inset in Fig. 1. When the applied voltage is positive the Mo/p-type a-Si:H junction is reverse biased whereas the p-type a-Si:H/SnO_2:F junction is forward biased. The opposite will occur for negative bias. In general, we expect that the current of the devices is dominated by the junction in reverse polarization. In Fig. 1 the measured J-V curve of the SnO_2:F/p-type a-Si:H/Mo device at 30 °C of a sample with diameter equal to 0.02 cm is reported. All J-V curves obey to cubic law $J = a \cdot V^3 + b \cdot V$ (red curve in Fig. 1). The measured J-V curves show two regions: in the range where $|V| < 0.1$ V the J-V is linear, whereas for $|V| < 0.1$ V it follows a power law. Since the J-V curve is almost symmetric, we conclude that the barrier heights of the two junctions are comparable.

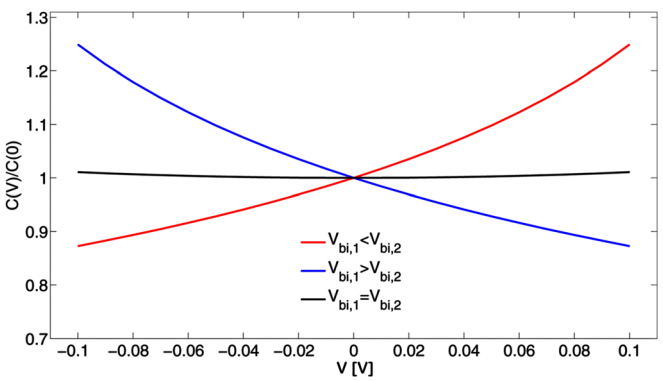

FIG. 2. (Color online) Theoretical C-V curves normalized to the value at 0 V obtained by using back to back model and for three different cases. If $V_{bi,1}$ is higher (blue) or smaller (red) than $V_{bi,2}$ the capacitance decreases or increases, respectively. If $V_{bi,1}$ is equal to $V_{bi,2}$ the capacitance is almost constant.

The impact of the voltage drop across the SnO_2:F layer and the presence of leakage currents has been investigated. This TCO has a good electrical performance but its conductivity is not as high as a metal and the contribution of the TCO to the series resistance might be important.[19] We have tested the leakage current and the TCO effects verifying the dependence of the J-V curves with the radius of the samples. We have found that the J-V curves do not depend on the area for the devices with diameters up to 0.08 cm.

Based on these analysis we have demonstrated that the J-V curves of the investigated devices with diameter smaller than 0.08 cm do not depend on the TCO sheet resistance. Then, we have chosen to analyze the devices with the smallest diameters, that is 0.02 and 0.04 cm.

To understand the transport mechanism we have analyzed several types of transport which are usually present in this type of heterojunctions. First, the diffusion and the recombination transport mechanisms of p-n junctions[18] are excluded because the J-V curves cannot be fitted by an exponential law in any voltage range. The following analyzed transport mechanism is the space charge limited current (SCLC).[20] The J-V curves, for $|V| < 0.1$ V, follow a power law $J = K \cdot V^m$, with the exponent $m > 2$ for $|V| < 0.2$ V. Thus, we may suppose that for $|V| < 0.2$ V the current is limited by the SCLC law in the p-type a-Si:H layer. In this case and if the exponential bandtails near the valence edge dominate, it yields $J \propto V^{(Tc/T)+1}$,[20,21] where T_C is the characteristic temperature, which depends on the width of the valence bandtails. Therefore, we could extract, in the power law region, T_C from the exponent $m = (T_C/T) + 1$. But the extracted characteristic temperature is not constant with the temperature so we conclude that the SCLC with exponential defects is not the dominant transport mechanism in this heterojunction at high bias voltages. Moreover, the comparison of the experimental J-V curves obtained on samples with 20 nm and 100 nm thick p-type a-Si:H films (not reported here) show very similar characteristics, so the observed negligible dependence on the thickness of the p-type a-Si:H layer rules out the SCLC mechanism.

Author complimentary copy. Redistribution subject to AIP license or copyright, see http://jap.aip.org/jap/copyright.jsp

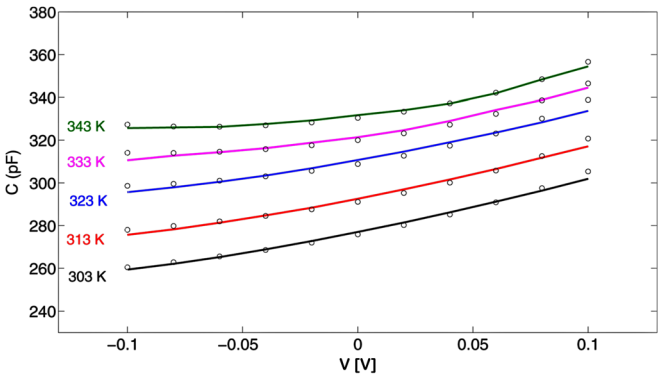

FIG. 3. (Color online) Comparison between the fitting (lines) by using C-V back to back model and the measurements (circles) capacitance of a sample of 0.02 diameter at different temperatures (from 303 to 343 K) by using a doping density extracted from J-V simulation with a barrier height of 0.49 eV *at* the Mo/p-type a-Si:H interface.

Figure 3 shows the measured C-V curves (circles) at different temperatures in the [−0.1, 0.1] V range. The C-V curve has been performed at high frequency (1 MHz) because the contribution of the depletion layer capacitance becomes dominant compared to that due to the interface states. We note that the capacitance increases with the voltage and based on the model (Eq. (1)), we can affirm that $\Delta V_{bi} = (V_{bi,2} - V_{bi,1}) > 0$. So the built in potential of the SnO_2:F/p-type a-Si:H heterojunction is greater than that of the Mo/p-type a-Si:H junction.

The experimental C-V data at various temperatures have been fitted to the model of Eq. (1) (continuous lines) with an excellent match. The best fit parameters are discussed in Sec. VI together with the analysis of the J-V characteristics.

V. COMPUTER SIMULATIONS OF THE SnO_2:F/P-TYPE a-Si:H HETEROJUNCTION

On the basis of the C-V analysis we can affirm that SnO_2:F/p-type a-Si:H has a barrier less transparent than that of the Mo/p-type a-Si:H junction. The slight asymmetry in the J-V curves confirms this difference. So we now focus on the heterojunction SnO_2:F/p-type a-Si:H.

We have used the one dimensional charge transport simulation program SCAPS 2.9.03 (Ref. 14) to analyze the transport mechanism of the SnO_2:F/p-type a-Si:H heterojunction and to define its band diagram. SCAPS 2.9.03 allows to insert the interface defects between the SnO_2:F and p-type a-Si:H layers. The parameters of these defects are the density, the type, the position, the energy distribution (Gaussian, exponential, etc.) and the capture cross section of holes and electrons. In particular, also the tunneling from (to) the trap levels to (from) the valence and conduction band edges can be simulated. This tunneling takes also into account the Poole-Frenkel effect and it is valid only for interface defects and not for bulk defects.

The simulated structure is implemented with two bulk layers, 20 nm of the p-type a-Si:H and 800 nm of SnO_2:F. The front contact with a-Si:H has been implemented with a barrier height $\phi_{B,1}$ and the back contact as ohmic. For the p-type a-Si:H and SnO_2:F layers we have used the input parameters proposed by Prentice[5] and Smole *et al.*[1] shown in Table I, which are the averaged values from a large variety of literature sources.

In this work we assume a Gaussian distribution acceptor-type defects at the interface between the SnO_2:F and p-type a-Si:H layers, with a capture electrons and holes cross sections of 9.0×10^{-16} and 1.0×10^{-14} cm^{-2}, respectively, and effective masses at the SnO_2:F/p-type a-Si:H interface similar to those of a-Si, that is, 0.3 for the holes[24] and 0.1 for the electrons.[25] For the SnO_2:F doping level we have used the value estimated from the resistivity measurements (2.9×10^{20} cm^{-3}), which is similar to the value used by Smole *et al.*[1] and supported by other experimental studies.[22,23] The free parameters in our simulations are the concentration of the acceptor-like states at the p-type a-Si:H/SnO_2:F interface $N_{G,\text{int}}$, their energy distribution width ΔE and peak position $E_D - E_V$, the doping of the p-type a-Si:H layer N_A and the barrier height of the Mo/p-type a-Si:H contact $\phi_{B,1}$.

Generally, the properties of the SnO_2:F/p-type a-Si:H interface are influenced by hydrogen related effects, by reactions between a-Si and TCO (Ref. 9) and by interface defect due to high Boron concentration.[1] Moreover, the potential barrier of the p-type a-Si:H is intimately related with the nature of the interface state concentration.[5] It was demonstrated that in SnO_2/p-type a-Si:H heterojunctions there is a band bending and a decreasing of the barrier potential due on interface states,[3] that could explain the measured high currents of the investigated structures (about 0.25 A/cm at $V = -0.2$ V). Hence, it is reasonable to attribute the reduction of the potential barrier, seen by the holes in the p-type a-Si:H at the p-type a-Si:H/SnO_2:F interface, to the negatively charged interface states, i.e., acceptor-like defects, as suggested by other authors.[1,5]

TABLE I. SCAPS 2.9.03 input parameters.

Parameters	SnO_2:F	p-type a-Si:H
Mobility gap, E_G [eV]	3.5	1.87
Relative dielectric permettivity, ε_r	9	11.8
Electron affinity, χ [eV]	4.8	3.9
Density of states, N_C, N_V, [cm^{-3}]	10^{21}	2.5×10^{20}
Electron band mobility, μ_e [cm^2/Vs]	30	10
Holes band mobility, μ_h [cm^2/Vs]	3	1
Conduction Band Tails		
Amplitude [cm^{-3}]	–	6.0×10^{19}
Slope, [meV]	–	40
Electron capture cross section, σ_n [cm^2]	–	2.1×10^{-17}
Holes capture cross section, σ_p [cm^2]	–	2.5×10^{-15}
Valence Band Tails		
Amplitude [cm^{-3}]	–	9.0×10^{19}
Slope, [meV]	–	59
Electron capture cross section, σ_n [cm^2]	–	2.5×10^{-15}
Holes capture cross section, σ_p [cm^2]	–	2.1×10^{-17}
Donor-like Dangling Bond		
Concentration [cm^{-3}]	–	3.6×10^{18}
Standard deviation [meV]	–	150
Electron capture cross section, σ_n [cm^2]	–	9.0×10^{-16}
Holes capture cross section, σ_p [cm^2]	–	1×10^{-14}
Distance from E_V [eV]	–	1,00

Author complimentary copy. Redistribution subject to AIP license or copyright, see http://jap.aip.org/jap/copyright.jsp

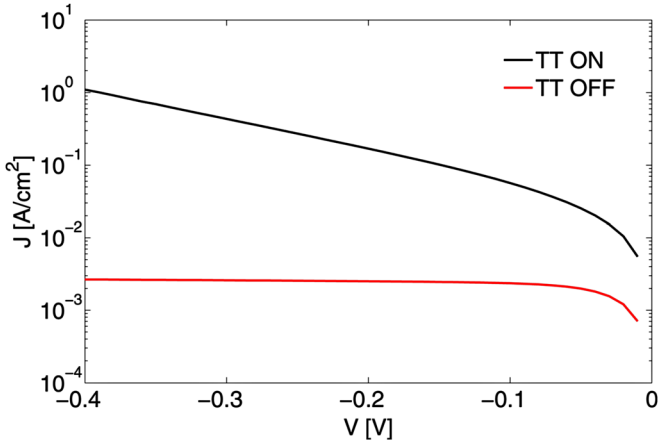

FIG. 4. (Color online) Comparison between simulated J-V curves with (black) and without (red) the activation of the option "allow tunneling to traps" (TT) in SCAPS software of the SnO_2:F/p-type a-Si:H heterojunction in reverse polarization.

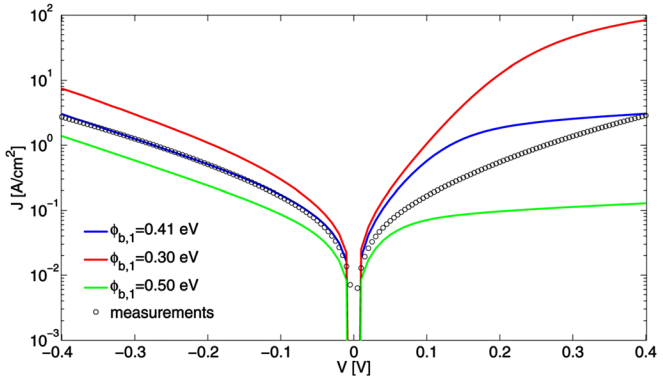

FIG. 5. (Color online) Comparison between the measured (black circles) and the simulated (lines) J-V curve at $T=313$ K of the SnO_2:F/p-type aSi:H/Mo structures, for different barrier heights. The values of the a-Si:H doping and of the interface defect density are $N_A=5.2\times10^{18}$ cm^{-3} and $N_{G,\text{int}}=4.1\times10^{13}$ cm^{-2}, respectively.

Prentice[5] has studied the effect of the acceptor-like surface states on the contact potential at the interface SnO_2/p-type a-Si:H. He found that, when the surface states are located at a fixed position in the gap, increasing their concentration $N_{G,\text{int}}$ resulted in a decrease of the barrier height seen by holes at the SnO_2:F/p-type a-Si:H interface. Moreover, he found that if the doping concentration N_A of the a-Si:H increases, the barrier height seen by holes in the p-type a-Si:H increases too, in the absence of any surface states. We have also tested these effects in our structure and we obtained the same results.

Firstly, we have tested the impact of tunneling on the emissivity of the interface traps. This is achieved by using the option of SCAPS "allow tunneling to traps" (TT) in the interface properties panel. Figure 4 shows the simulated reverse current of the SnO_2:F/p-type a-Si:H junction obtained by using $N_{G,\text{int}}=4.0\times10^{13}$ cm^{-2}, $\Delta E=0.15$ eV, $E_D-E_V=0.4$ eV, $N_A=5.2\times10^{18}$ cm^{-3} and $\phi_{B,1}=0.41$ eV at $T=300$ K with and without the activation of the TT option. We note that with the activation of the TT option the reverse current increases of some magnitude orders, in agreement with the experimental results, with a physically plausible set of parameters, and with a stronger dependence on the reverse voltage. By considering the J-V characteristics experimentally found, we propose that the transport mechanism for this SnO_2:F/p-type a-Si:H heterojunction is the tunnel generation (recombination) of electron/hole pairs from (to) interface defects to (from), respectively, SnO_2:F conduction band and p-type a-Si:H valence band.

VI. RESULTS AND DISCUSSION

Figure 5 shows the experimental J-V curves of the SnO_2:F/p-type a-Si:H heterojunction at $T=313$ K and the simulated J-V curves calculated by using $N_{G,\text{int}}=4.1\times10^{13}$ cm^{-2}, $\Delta E=0.15$ eV, $E_D-E_V=0.4$ eV, $N_A=5.2\times10^{18}$ cm^{-3} at different values of the barrier height $\phi_{B,1}$, with the bias voltage varying from -0.4 to $+0.4$ V. We note that, when $\phi_{B,1}=0.41$ eV, the simulated curve fits well the experimental data only for negative voltages. The simulated J-V curves for positive voltages show a different functional dependence on the voltage compared to the experimental data. We explain this behavior by considering that the measured current for positive voltage is dominated by the reverse current of the Mo/p-type a-Si:H junction. By increasing the barrier height $\phi_{B,1}$ we obtain only the reduction of the current for both positive and negative voltages and the simulated curve for positive voltages does not obey the cubic law observed in the measured J-V curves. Moreover, if we increase the doping density at a fixed value of the barrier height $\phi_{B,1}$, the simulated J-V curves increase maintaining the same functional dependence for both positive and negative voltages. Thus, the proposed model (tunnel assisted generation of electron/hole pairs) is able to explain well the experimental data only for negative bias, but not for positive voltages because in this case the junction Mo/p-type a-Si:H dominates. Indeed, the possible values of $\phi_{B,1}$, ΔE, E_D-E_V, and N_A are not unique. However, the consistency with the experimental data poses strong constraints so that the set of physically acceptable parameters is uniquely determined. In particular, as far as the values of $\phi_{B,1}$ and N_A are concerned, we have chosen the values that allow at the same time to fit the measured C-V and J-V curves at the various temperatures. The "best-fit" values of $V_{bi,1}$, $V_{bi,2}$, N_A, $N_{G,\text{int}}$, E_D-E_V, and ΔE consistent with the experimental J-V and C-V data for different samples and obtained from both the simulated J-V curves and the capacitance model at $T=313$ K, are 0.14 ± 0.01 V, 0.16 ± 0.01 V, $5.6\pm0.2\times10^{18}$ cm^{-3}, $4.0\pm0.2\times10^{13}$ cm^{-2}, 0.40 eV, and 0.15 eV, respectively. The parameter variations at different temperatures are small ($<7\%$). Figure 6 shows the experimental (black circles) and the best fit simulated (red lines) J-V curves at different temperatures. Figure 3 shows the experimental C-V curves (black circles) at different temperatures together with the best fit (red lines) calculated according to the C-V model of Eq. (1).

We note that $V_{bi,2}$ is slightly larger than $V_{bi,1}$, hence we conclude that the defects at the respective interfaces may have a similar origin and close features. These defects could be generated by the oxidation of the p-type a-Si:H surfaces, which occurs when it puts in contact with the metal and the

Author complimentary copy. Redistribution subject to AIP license or copyright, see http://jap.aip.org/jap/copyright.jsp

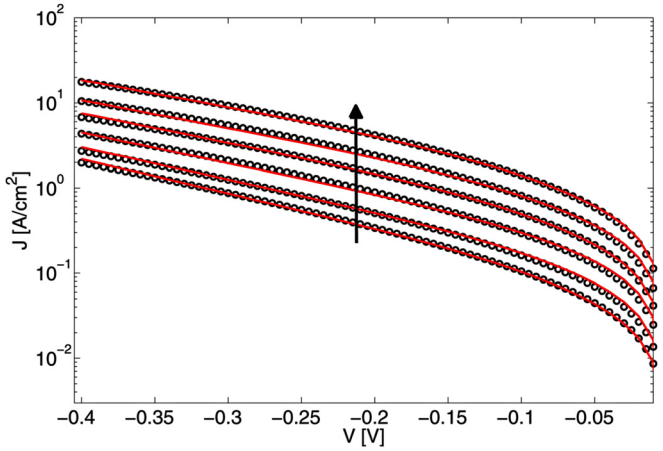

FIG. 6. (Color online) Simulated (red lines) and measured (black circles) J-V curves for negative voltages of the p-type a-Si:H/SnO_2:F heterojunction at different temperatures (from 303 to 353 K). The simulation curve are obtained by using a barrier height of 0.49 eV at the Mo/p-type a-Si:H, a interface defect density of 4.0×10^{13} cm^{-2} at the SnO_2:F/p-type a-Si:H and a doping density of the p-type a-Si:H of 5.6×10^{18} cm^{-3}. The arrow indicates the increase of the temperatures.

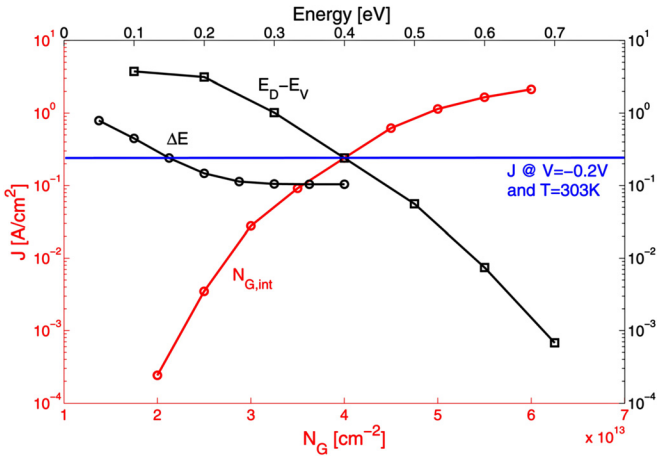

FIG. 7. (Color online) Simulated Current Density at $V = -0.2$ V and $T = 303$ K for different width ΔE (circle black) and position $E_D - E_V$ (square black) and for different defect density N_g (circle red) of the heterostructure SnO_2:F/p-type a-Si:H/Mo. In blue the measured current density J at $V = -0.2$ V and $T = 303$ K.

SnO_2:F.[26] Moreover, the molybdenum and the SnO_2:F have similar work function (close to 4.8 eV).[1,18]

To better understand how the interface defect parameters influence the simulated current density, we performed a sensitivity analysis. As starting set we use the parameter value group obtained from the best fitting of the C-V and I-V characteristics above described. We only varied the interface defects properties as the distribution width ΔE, the peak position $E_D - E_V$ and the density $N_{G,\text{int}}$.

In Fig. 7 the variation of the reverse current density of the SnO_2:F/p-type a-Si:H heterojunction at a fixed voltage $V = -0.2$ V and $T = 303$ K for different values of $E_D - E_V$ (square black), ΔE (circle black) and $N_{G,\text{int}}$ (circle red) are shown. The measured current density value is evidenced by the blue line. In particular, for a variation of the distribution width from 0.05 to 0.4 eV the current goes from 0.7 to 0.1 A/cm and saturates beyond 0.3 eV. For a variation of the position peak from 0.2 eV to 0.6 eV above the p-type a-Si:H valence band the current density goes from 3.0 A/cm^2 to 6.0×10^{-3} A/cm^2. The reverse current density is very sensitive to the value of the defect density $N_{G,\text{int}}$. In fact a variation of $N_{G,\text{int}}$ from 2.0 to 6.0×10^{13} cm^{-2}, the current density goes from 2.0×10^{-4} to 2.0 A/cm^2.

When the defect distribution position approaches the p-type a-Si:H valence bandedge the reverse current density increases, because the barrier seen by the holes tunneling from the interface defect to the p-type a-Si:H valence band, is thinner and lower. Hence, it is the hole current which limits the transport charge in the heterojunction SnO_2:F/p-type a-Si:H. The current density variation due to the width of the Gaussian interface distribution is due to the change in the energy position of the defects. From Fig. 7 it is evident that the interface defects peak position and density have a strong effect on the value of the current density. This implies that the range of the space parameters consistent with the measured current densities is quite narrow. Further restrictions are given by physical plausibility. The chosen interface parameters used in this work are in agreement with those used by Prentice[5] and allow to obtain plausible physical values of the other parameters to fit the experimental data. For example, if we consider a defect energy positions larger than 0.4 eV we have to insert a defect density greater than 10^{14} cm^{-2}.

From the previous analysis we conclude that the main reverse transport mechanism of the SnO_2:F/p-type a-Si:H heterojunction for negative bias is the tunnel assisted generation of holes and electrons from interface defects to, respectively, the valence bandedge of the a-Si:H and the conduction bandedge of SnO_2:F. Moreover, we think that the limiting transport is that of the holes (not of the electrons), justified by the lower hole mobility, due to the wider Urbach tail,[24] and even suggested by the high dependence of the current density on the distance of the defects position from the p-type a-Si:H valence bandedge (see Fig. 7). The trap-assisted tunneling carrier capture and emission has already been proposed to model the transport mechanism in a-Si p-n homojunctions,[27] and different approaches exist to model this mechanism.[28,29] Moreover, this mechanism allows also to explain the current transport in amorphous silicon n/p tunnel junctions present in tandem solar cells.[30]

Given the similar J-V characteristic for positive voltages, we can suppose that also the reverse current of the Mo/p-type a-Si:H junction is governed by a similar transport mechanism as the one above proposed for the SnO_2:F/p-type a-Si:H junction.

The high defects density at the SnO_2:F/p-type interface depends mainly on the physical and chemical reaction during and after the a-Si:H deposition. The SnO_2:F of the investigated structure is a commercial TCO, widely used as front contact in thin film photovoltaic modules, hence is mainly the growth process of the p-type a-Si:H on the TCO which determines the interface properties. In fact, other authors suggested that the high current at this interface can be due to tunneling through thin spot or possible conducting deposits in the p-type layer.[3] For these reasons we think that the transport mechanism through acceptor interface defects is valid

Author complimentary copy. Redistribution subject to AIP license or copyright, see http://jap.aip.org/jap/copyright.jsp

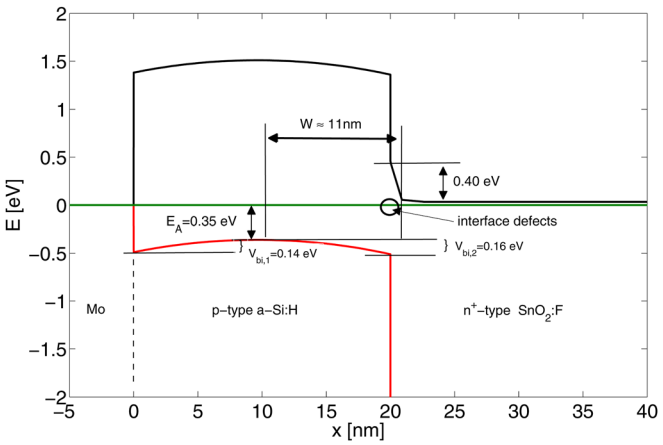

FIG. 8. (Color online) Simulated energy band diagram of the heterojunctions SnO_2:F/p-type a-Si:H with a Gaussian surface state density of 4.0×10^{13} cm^{-2}, 0.4 eV above the valence bandedge of the p-type a-Si:H layer at $T = 30\,^{\circ}C$ and with a doping density of 5.6×10^{18} cm^{-3}.

not only for SnO_2/p-type a-Si:H heterojunctions but also for other TCO/p-type a-Si:H heterojunctions. For example, Smole *et al.*[1] found that an high acceptor-like interface state density causes an band bending at the interface and, hence an increasing of the current density for both SnO_2:F/p-type a-SiC:H and ZnO/p-type a-SiC:H heterojunctions.

The model here described suggests that to improve the TCO performances for the contact resistance it is needed to increase the acceptor-like defect density at the interface by using a careful surface preparation and a greater concentration of boron atoms in the p-type a-Si:H layer.[1]

As summary, Fig. 8 shows the simulated band diagram of the SnO_2:F/p-type a-Si:H heterojunction at $T = 30\,^{\circ}C$ and $V = 0$ V. The p-type a-Si:H depletion width is about 10 nm, while it is about 1 nm at the SnO_2:F side. From this band diagram we derived a value of 0.35 eV for the activation energy of the a-Si:H layer, in agreement with the measured value of 0.38 eV. The barrier height at the SnO_2:F/p-type a-Si:H interface is 0.51 eV. This value of barrier height is similar to that found by Itoh,[4] which determined a barrier height of 0.56 eV for SnO_2/p-type a-SiC and by Sinencio,[3] which found 0.66 eV for SnO_2/p-type a-Si:H. Both authors supposed that the SnO_2/a-Si:H junction is a Schottky contact governed by thermionic emission. We on the contrary find evidence that the transport is due to tunnel assisted generation of electron/hole pairs from interface defects.

VII. CONCLUSIONS

In summary, in this work we have performed an accurate electrical characterization of the SnO_2:F/p-type a-Si:H/Mo structure, which allows us to make a detailed phenomenological modeling of the SnO_2:F/p-type a-Si:H heterojunction.

After having excluded some common transport mechanisms such as diffusion, generation-recombination and SCLC, we have concluded that the SnO_2:F/p-type a-Si:H/Mo structure can be considered as composed by two junctions back to back connected. We have proposed an analytical model of the C-V characteristics of these series connected junctions. The J-V characteristics are dominated in all cases by the transport bottle-neck, individuated as the reverse bias transport of the SnO_2:F/p-type a-Si:H and p-type a-Si:H/Mo junction, respectively, for negative and positive voltages of the Mo/p-type a-Si:H/SnO_2:F structure. With the use of the simulation software SCAPS we demonstrate that the transport in the SnO_2:F/p-type a-Si:H heterojunction for reverse bias is attributed to generation of electron/hole pairs and subsequent electrons and holes tunneling from interface defects to SnO_2:F conduction band and a-Si:H valence band, respectively. The holes tunneling is the transport bottle-neck which limits the total current of the structure.

Then, we have performed the fitting of the simulated J-V and analytical C-V curves to the experimental data at different temperatures. The obtained parameters, at 303 K, are a high acceptor-like interface defects density of $4.0 \times 10^{13}\,cm^{-2}$ at the SnO_2:F/p-type a-Si:H interface, a doping density of 5.6×10^{18} cm^{-3} of the p-type a-Si:H layer and built-in potentials of 0.14 V and 0.16 V for the Mo/p-type a-Si:H and SnO_2:F/p-type a-Si:H, respectively. A sensitivity analysis on distribution width ΔE, peak position $E_D - E_V$ and the density $N_{G,\mathrm{int}}$ of the Gaussian distribution interface defects is performed and a band diagram of the SnO_2:F/p-type a-Si:H/Mo structure at 0 V and 30 °C is proposed.

ACKNOWLEDGMENTS

This work has been carried out with the partial support by the University of Palermo through the ex-60% funds and by STMicroelectronics. We gratefully acknowledge the team of STMicroelectronics (S. Coffa, S. Ravesi, N. Sparta) for the help in the research development. The authors would also like to thank M. Burgelman and K. Decock of the University of Gent for the valuable discussions on the SCAPS 2.9.03 software.

[1] F. Smole, M. Topic, and J. Furlan, J. Non-Cryst. Solids **194**, 312 (1996).
[2] D. Rached and R. Mostefaoui, Thin Solid Films **516**, 5087 (2008).
[3] F. Sanchez Sinencio and R. Williams, J. Appl. Phys **54**(5), 2757 (1983).
[4] K. Itoh, H. Matsumoto, T. Lobata, and A. Fujishima, Appl. Phys. Lett. **51**, 1685 (1987).
[5] J. S. C. Prentice, J. Non-Cryst. Solids **262**, 99 (2000).
[6] V. A. Dao, J. Heo, H. Choi, Y. Kim, S. Park, S. Jung, N. Lakshminarayan, and J. Yi, Sol. Energy **84**, 777 (2010).
[7] F. Einsele, P. J. Rostan, and M. B. Schubert, J. Appl. Phys. **102**, 094507 (2007).
[8] R. Gordon, MRS Bull., **25**, 52 (2000).
[9] H. Stiebig, F. Siebke, W. Beyer, C. Benekin, B. Rech, and H. Wagner, Sol. Energy Mater. Sol. Cells **48**, 351 (1997).
[10] A. Alkaya, R. Kaplan, H. Canbolat, and S. S. Hegedus, Renewable Energy **34**, 1595 (2009).
[11] H. Shade, Z. E. Smith, J. R. Thomas III, and A. Catalano, Thin Solid Films **117**, 149 (1994).
[12] W. B. Jackson, R. J. Nemanich, M. J. Thompson, and B. Wacker, Phys. Rev. B **33**, 6936 (1986).
[13] K. J. B. M. Nieuwesteeg, M. Van der Veen, T. J. Vink, and J. M. Shannon, J. Appl. Phys. **74**, 2581 (1994).
[14] M. Burgelman, P. Nollet, and S. Degrave, Thin Solid Films, **361–362**, 527 (2000).
[15] G. Cannella, F. Principato, M. Foti, C. Garozzo, and S. Lombardo, Energia Procedia **3**, 51 (2011).
[16] S. Pandey and S. Kal, Solid-State Electron. **42**, 943 (1998).
[17] P. Chattopadhyay, Solid-State Electron. **39**, 1491 (1996).

Author complimentary copy. Redistribution subject to AIP license or copyright, see http://jap.aip.org/jap/copyright.jsp

[18]S. M. Sze, *Physics of Semiconductor Devices*, 2nd ed. (Wiley Interscience, New York, 1981).
[19]F. Principato, G. Cannella, M. Foti, and S. Lombardo, Solid-State Electron. **54**, 1284 (2010).
[20]A. Rose, Phys. Rev. **97**, 1538 (1955).
[21]S. Ashok, A. Lester, and S. J. Fonash, IEEE Elec. Dev. Lett. **EDL-1**, 200 (1980).
[22]Z. Crnjak Orel, B. Orel, and M. Klanjsek Gunde, Sol. Energy Mater. Sol. Cells **26**, 105 (1992).
[23]A. Antonaia, P. Menna, M. L. Addonizio, and M. Crocchialo, Sol. Energy Mater. Sol. Cells **28**, 167 (1992).
[24]R. A. Street, *Hydrogenated Amorphous Silicon* (Cambridge University Press, New York, 1991).
[25]J. M. Shannon, Appl. Phys. Lett. **62**, 1815 (1993).
[26]M. Kubon, E. Boehmer, F. Siebke, B. Rech, C, Beneking, and H. Wagner, Sol. Energy Mater. Sol. Cells **41/42**, 485 (1996).
[27]J. Furlan, Prog. Quantum Electron. **25**, 55 (2001).
[28]G. Vincent, A. Chantre, and D. Bois, J. Appl. Phys. **50**, 5484 (1979).
[29]G. A. M. Hurkx, D. B. M. Klaassen, and M. P. G. Knuvers, IEEE Trans. Elect. Dev. **39**, 331 (1992).
[30]S. S. Hegedus, F. Kampas, and J. Xi, Appl. Phys. Lett. **67**(6), 813 (1995).

Author complimentary copy. Redistribution subject to AIP license or copyright, see http://jap.aip.org/jap/copyright.jsp